Development of a Fluence Generating Programme for Patient-Specific Quality Assurance and Calibration of an Amorphous Silicon EPID

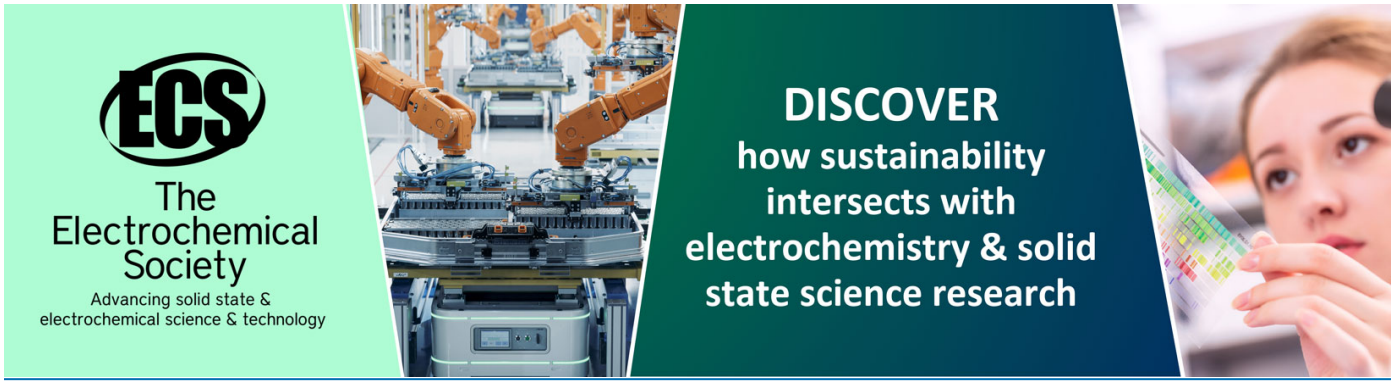

Development of a Fluence Generating Programme for Patient-Specific Quality Assurance and Calibration of an Amorphous Silicon EPID

C F Yeap[1], W L Jong[2] and N M Ung[2]

[1]Department of Biomedical Imaging, Faculty of Medicine, University of Malaya, Kuala Lumpur, Malaysia
[2]Clinical Oncology Unit, Faculty of Medicine, University of Malaya, Kuala Lumpur, Malaysia

wljong88@um.edu.my

Abstract. Patient-specific quality assurance (QA) is an essential part of intensity-modulated radiotherapy (IMRT) and volumetric arc therapy (VMAT) treatments. This study aims to develop a Patient-specific QA system through the development of a fluence generating programme and utilization of amorphous silicon (aSi) electronic portal imaging device (EPID). The EPID was investigated on the dependency of dose rate, uniformity of detector sensitivity and output factor. A fluence generating programme was written using MATLAB. Five simple dynamic arc plans and one patient VMAT plan were created using the Monaco treatment planning system which were used in the programme to generate fluence maps. The accuracy of the programme was evaluated by performing gamma analysis between the generated and measured fluence. EPID signal was found to be linearly proportional to dose (1-1000 MU) and independent of dose rate. The mean uniformity ratio was 1.07 ± 0.04%. The measured fluence maps were corrected for uniformity before gamma analysis. Output factor and dose deposition were taken into account in the process. The average result of the gamma analysis passed the 95% threshold. A fluence generating programme was developed, serving as the foundation of the Patient-specific QA system using aSi EPID for IMRT/VMAT delivery in this centre.

1. Introduction

The Patient-specific QA is an important part of the IMRT, it ensures the accuracy of dose delivery due to the high complexity of fields. EPID, which is incorporated with LINAC is used for setup verification purpose. It was first used in 1991 for dose measurement [1] and the characterization was done in various studies [2]. EPID was reported to be independent of gantry angle [3] and can be used interchangeably with 2D or 3D arrays [3-5]. It also has a higher spatial resolution [6] and high image contrast [7]. Amorphous silicon (aSi) based EPID is the most commonly used EPID nowadays [2].

PortalVision system developed by Varian (Varian Medical Systems, Palo Alto, CA, USA) enables the use of EPID for patient-specific QA. However, this functionality is not available for some other systems. Hence, centres with such systems may benefit from the development of a fluence generating program. Performing Patient-specific QA using EPID requires two components: the predicted response of EPID to energy fluence of the treatment and a calibrated EPID. For simplicity, the response of EPID to energy fluence will be represented as “fluence” in this article.

The raw fluence generated from the multi-leaf collimator (MLC) positions should be convolved with a dose deposition kernel to consider the scattering and optical glare of EPID. There are different methods of obtaining the kernel, however, the most commonly used method is the Monte Carlo simulation. This study investigated three aspects of aSi EPID: dose rate, uniformity and output factor. Several studies have concluded that aSi EPID response is non-linear to dose rate [15-17]. However, these findings were inconsistent [18] and was addressed by Alshanqity and Nisbet [19]. Their study found that signal per MU is not influenced by dose rate. The effect of dose rate only contributed up to 2.1% to the total signal as residual signal. The uniformity of detector response was corrected by performing flood field correction but this method only corrected the detector response to the average response of all detectors. An improved flood field calibration method [20] was proposed and tested in several other studies. The pixel gain factors obtained were in the range of 0.9 to 1.1 [21] and 0.93 to 1.06 [22]. Finally, output factor was taken into consideration since it can be larger than 1.10 for field sizes larger than 25×25 cm^2 [18, 23, 24].

2. Materials and Methods

The LINAC used in this study is Elekta Versa HD (Elekta AB, Stockholm, Sweden) which is equipped with Elekta Agility MLC. The LINAC was incorporated with an EPID based on aSi detector panel, model XRD 1640 AL5 (PerkinElmer Optoelectronics, Fremount, CA, USA). The detector was fixed at a source-to-surface distance (SSD) of 160 cm. The radiation sensitive area was 40.96×40.96 cm^2, consisting of 1024×1024 pixels. This dimension is equivalent to 25.9×25.9 cm^2 at SSD 100 cm. 1 mm of copper was placed on the detectors as build-up material. A detailed structure and detection mechanism of aSi detectors can be found in articles [25-28].

Five simple single full dynamic arc plans with 200 MU each, were created to test the system. The plans were of geometric shapes (5×5 cm^2 and 10×10 cm^2 squares, circle and diamond) and had no modulation of MLC except for one of the plans which had a simple transition from one shape to another. A real patient's head and neck VMAT plan was also used to be compared with the simple plans.

2.1. Calibration of EPID

The images acquired using iViewGT software (Elekta AB, Version 3.4.1) needed to be modified from the averaged pixel values to the integrated pixel value using Equation (1) as in [29]:

$$\text{Integrated Pixel Value (IPV)} = \frac{65535 - Raw\ Pixel\ Value}{Pixel\ Scaling\ Factor} \quad (1)$$

The *pixel scaling factor (PSF)* in Equation (1) can be obtained from the log file of each EPID image. All images were acquired using the "single exposure" option and was saved in the "tiff" format. A 10×10 cm^2 field was irradiated with 6 MV photon beam from 1 to 1000 MU at a fixed dose rate of 600 MU/min. Conversion to IPV was done using MATLAB (The MathWorks Inc, Version 8.3.0.532 (R2014a)). The mean IPV of central 3×3 cm^2 was calibrated to the corresponding MU.

2.1.1. Dose rate. Since Elekta Versa HD only allows irradiation at certain dose rates: 100, 200, 300, 600 MU/min, only these dose rates were used. The first test involved varying the dose rates while keeping a constant 100 MU. Then, to eliminate the effect of the irradiation duration on the EPID response, the measurement was repeated using the same set of dose rates with a constant irradiation time of 30 s and varied MU.

2.1.2. Uniformity. Based on the method in [20], a 100 MU of 25×25 cm^2 was delivered at three different positions respectively: at zero shift, 2 cm shift to the left and 2cm shift to the right. The obtained images were then shifted back to the central axis using MATLAB. The average pixel value of two shifted images were calculated and normalized to the pixel value of non-shifted image at each point to obtain the uniformity correction factor. The result was a 1024×1024 uniformity mask.

2.1.3. Output factor. 100 MU was irradiated for different field sizes ranging from 2×2 to 25×25 cm^2. The maximum field size of EPID projected at isocentre plane is also only 26×26 cm^2. Mean IPVs of different field sizes were normalized to that of 10×10 cm^2 to obtain output factor. Output factor was plotted as a function of field size.

2.2. Fluence generating programme

The overall flow of procedure from fluence generation to gamma analysis between generated and measured fluence is shown in Figure 1. Fluence map for each control point was generated, convolved with an optimized dose deposition kernel [30] and corrected for output factor before being added to the final composite fluence. The kernel includes both scattering and optical glare and takes the form of

$$y = \exp(-a_1 r) + (a_2)\exp(-a_3 r) + (a_4)\exp(-a_5 r) \quad (2)$$

where r is the distance in pixel. The optimized coefficients in this study is a_1= 1.27 pixel^{-1}, a_2= 0.0008, a_3= 0.10156 pixel^{-1}, a_4= 0.0000175 and a_5= 0.0091404 pixel^{-1}. A lookup table was created based on the data collected in Section *2.1.3*. Output factor for each control point can be obtained using the lookup table and equivalent square field [31] of the control point.

The measured fluence from EPID requires modification using MATLAB to convert raw pixel values to MU detected using the calibration curve in Section *2.1*. Uniformity in Section *2.1.2* was also corrected. Both generated and measured fluence were compared using gamma analysis (3%/3 mm) in DoseLab Pro (Mobius Medical System, Version 7.0.0 Beta).

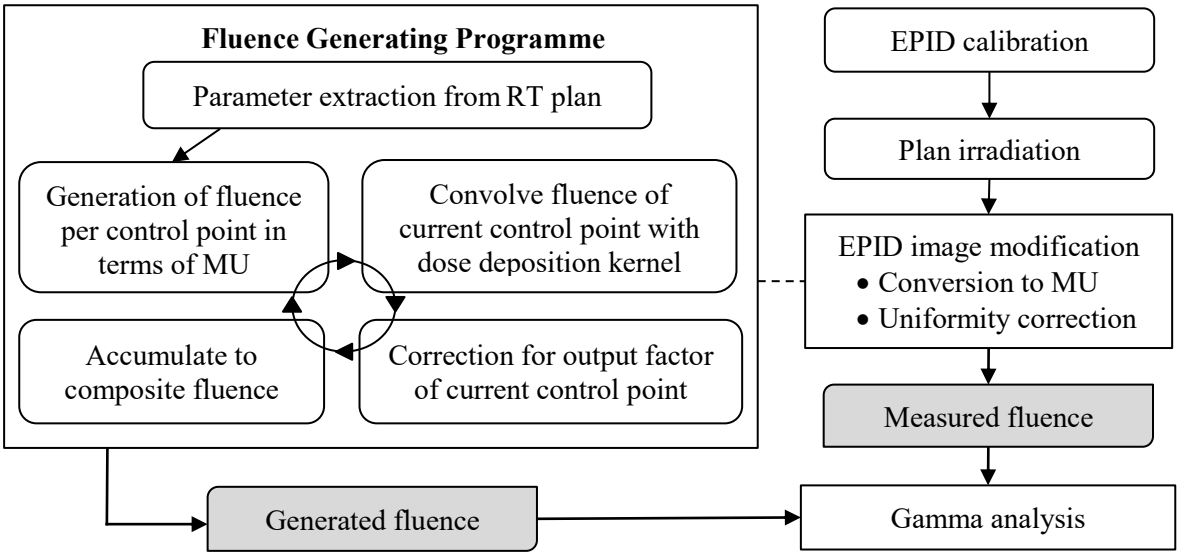

Figure 1: Overall flow of procedure.

3. Results and Discussion

3.1. Calibration of EPID

The results for calibration and output factor (Figure 2 and 3) in this study are coherent with other studies [18, 19, 23]. Coefficient of variations for all characterization tests are only up to 0.5%. The average value of uniformity correction factors is 1.0713 ± 0.04% with a maximum value of 1.0853.

Signal of EPID was found to be linear to dose rate in both tests ($R^2 \geqslant 0.95$ for linear fitting). In Winkler's study [17], it was found that the sensitivity of EPID increased up to 1.5% as the dose rate was doubled whereas the current study found the maximum increment to be 0.4%. The inconsistency in the findings could be due to the short readout time in some studies as discussed by Alshanqity [19] and quantification of signal. The quantity used for EPID signal in this study, IPV, is dependent on PSF which is inversely proportional to the MU delivered on independent dose rate.

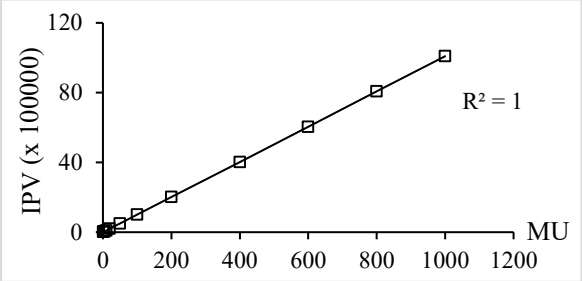

Figure 2: Calibration curve of aSi EPID.

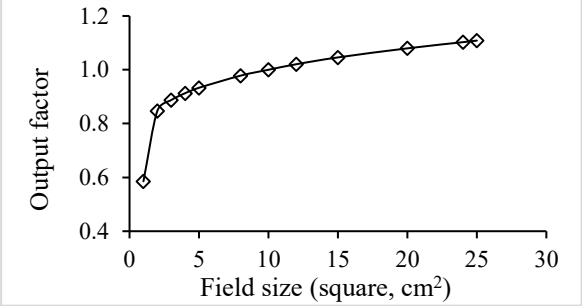

Figure 3: Output factor as a function of equivalent square field.

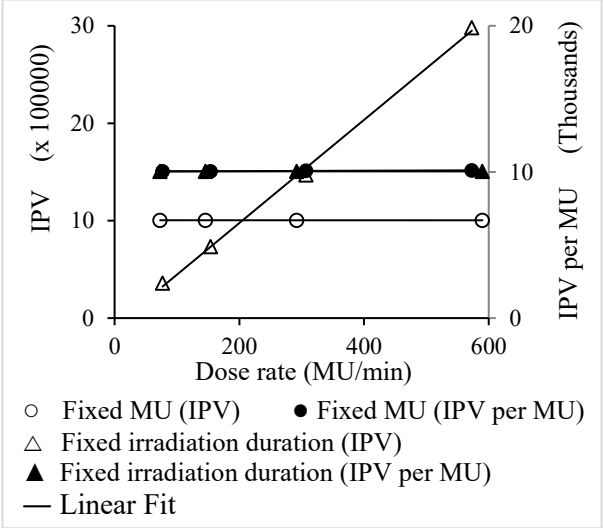

Figure 4: IPV and IPV per MU as a function of dose rate for fixed irradiated MU and fixed irradiation duration. Linear relationships were observed in both methods of variating dose rate. IPV is affected only by change of irradiated MU.

3.2. Gamma analysis result of generated and measured fluence

The generated fluences are as shown in Figure 6. The result of gamma analysis is shown in Table 1. The average gamma passing rate of all the plans tested passed the 95% threshold. However, not all plans can achieve 95%. Hence, the coefficients in Equation (2) still require further optimization to increase the accuracy of prediction of penumbra region as shown in Figure 5.

Table 1: Gamma passing rate between generated and measured fluence of all plans tested.

Plan	Gamma passing rate (%)
5x5 cm^2	95.8
10x10 cm^2	93.3
Circle	95.4
Diamond	96.3
Diamond-to-circle	99.5
Patient Plan	93.4
Mean	95.6
Standard Deviation	2.08

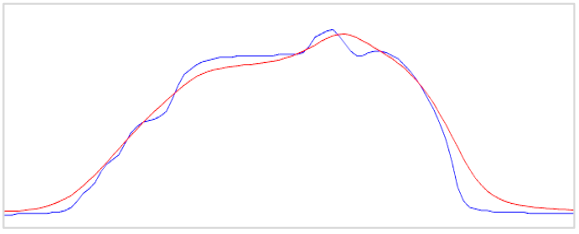

Figure 5: One of the cross-plane profile for patient plan fluence comparison. The generated fluence (blue) has shorter penumbra than the measured fluence (red).

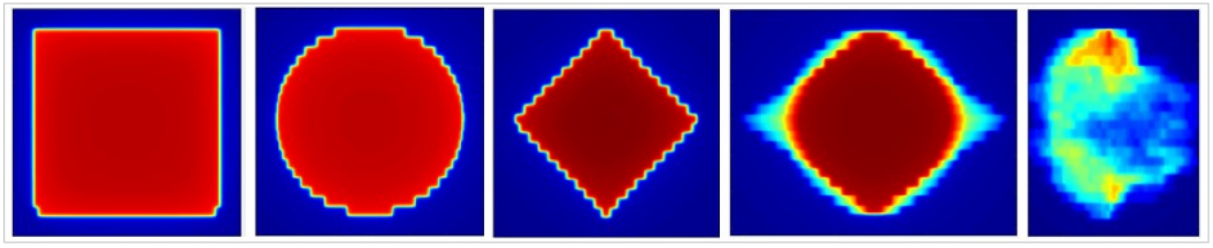

Figure 6: Generated fluence using the in-house programme: (from left to right) square, circle, diamond, diamond-to-circle and patient plan.

4. Future development

There are still many aspects of the programme that require improvement. Apart from the dose deposition kernel, other factors such as MLC transmission factor and TERMA (assumed to be 1cGy/MU in this study) should also be taken into consideration. More setup parameters can also be included in the fluence generation. For instance, angle of collimator and angle of couch and source-to-surface distance. The programme should not be limited to a certain brand of LINAC only. An in-house gamma analysis programme would be beneficial because the software used in this study has limitation in shifting and cropping the image. The last stage of development would be transitioning to a more user-friendly interface.

5. Conclusion

Calibration of EPID was done. Development of a Patient-specific QA system using aSi EPID was initiated with the development of a fluence generating programme. However, further improvement of the programme is necessary to achieve the required standard.

Acknowledgements

The first author would like to express gratitude towards SEAFOMP for the travel grant received.

References

[1] van Herk M 1991 Physical aspects of a liquid-filled ionization chamber with pulsed polarizing voltage *Med Phys* **18** 692-702
[2] Van Elmpt W, McDermott L, Nijsten S, Wendling M, Lambin P and Mijnheer B 2008 A literature review of electronic portal imaging for radiotherapy dosimetry *Radiother Oncol* **88** 289-309
[3] Sharma D S, Mhatre V, Heigrujam M, Talapatra K and Mallik S 2010 Portal dosimetry for pretreatment verification of IMRT plan: a comparison with 2D ion chamber array *J Appl Clin Med Phys* **11** 238-248
[4] Son J, Baek T, Lee B, Shin D, Park S Y, Park J, Lim Y K, Lee S B, Kim J and Yoon M 2015 A comparison of the quality assurance of four dosimetric tools for intensity-modulated radiation therapy *Radiol Oncol* **49** 307-313
[5] Krishna Murthy K 2012 Patient-specific quality assurance of RapidArc treatments: portal prediction dosimetry compared with phantom studies *Biomed Imaging Interv J* **8** e28-e34
[6] Hussein M, Adams E J, Jordan T J, Clark C H and Nisbet A 2013 A critical evaluation of the PTW 2D-ARRAY seven29 and OCTAVIUS II phantom for IMRT and VMAT verification *J Appl Clin Med Phys* **14** 274-292
[7] Allen B, Marcu L and Bezak E 2012 *Biomedical Physics in Radiotherapy for Cancer* (Clayton: Csiro Publishing) 149-150.
[8] Li W, Siebers J V and Moore J A 2006 Using fluence separation to account for energy spectra dependence in computing dosimetric EPID images for IMRT fields *Med Phys* **33** 4468-4480
[9] Chang J, Mageras G S, Ling C C and Lutz W 2001 An iterative EPID calibration procedure for dosimetric verification that considers the EPID scattering factor *Med Phys* **28** 2247-57
[10] Khan R F, Ostapiak O Z and Szabo J J 2008 An empirical model of electronic portal imager response implemented within a commercial treatment planning system for verification of intensity-modulated radiation therapy fields *J Appl Clin Med Phys* **9** 135-150
[11] Steciw S, Warkentin B, Rathee S and Fallone B G 2005 Three-dimensional IMRT verification with a flat-panel EPID *Med Phys* **32** 600-12
[12] Warkentin B, Steciw S, Rathee S and Fallone B G 2003 Dosimetric IMRT verification with a flat-panel EPID *Med Phys* **30** 3143-55
[13] Herwiningsih S, Hanlon P and Fielding A 2014 Sensitivity of an Elekta iView GT a-Si EPID model to delivery errors for pre-treatment verification of IMRT fields *Australas Phys Eng Sci Med* **37** 763-70

[14] McCurdy B M, Luchka K and Pistorius S 2001 Dosimetric investigation and portal dose image prediction using an amorphous silicon electronic portal imaging device *Med Phys* **28** 911-24
[15] McDermott L N, Louwe R J W, Sonke J J, Van Herk M B and Mijnheer B J 2003 Dose-response and ghosting effects of an amorphous silicon electronic portal imaging device *Med Phys* **31** 285-295
[16] McDermott L N, Nijsten S M, Sonke J J, Partridge M, van Herk M and Mijnheer B J 2006 Comparison of ghosting effects for three commercial a-Si EPIDs *Med Phys* **33** 2448-51
[17] Winkler P, Hefner A and Georg D 2005 Dose-response characteristics of an amorphous silicon EPID *Med Phys* **32** 3095-105
[18] Sukumar P, Padmanaban S, Jeevanandam P, Kumar S A S and Nagarajan V 2011 A study on dosimetric properties of electronic portal imaging device and its use as a quality assurance tool in volumetric modulated arc therapy *Rep Pract Oncol Radiother* **16** 248-255
[19] Alshanqity M and Nisbet A 2016 Dosimetric performance of a-si electronic portal imaging devices *International Journal of Medical Physics, Clinical Engineering and Radiation Oncology* **5** 162-175
[20] Boriano A, Lucio F, Calamia E, Russi E and Marchetto F 2013 A new approach for the pixel map sensitivity (PMS) evaluation of an electronic portal imaging device (EPID) *J Appl Clin Med Phys* **14** 234-250
[21] Cai B, Goddu S M, Yaddanapudi S, Caruthers D, Wen J, Noel C, Mutic S and Sun B 2018 Normalize the response of EPID in pursuit of linear accelerator dosimetry standardization *J Appl Clin Med Phys* **19** 73-85
[22] Sun B, Yaddanapudi S, Goddu S M and Mutic S 2015 A self-sufficient method for calibration of Varian electronic portal imaging device *J Phys Conf Ser* **573** 1-4
[23] Van Esch A, Depuydt T and Dominique P H 2004 The use of an aSi-based EPID for routine absolute dosimetric pre-treatment verification of dynamic IMRT fields *Radiother Oncol* **71** 223-234
[24] Van Esch A, Dominique P H, Hirschi L, Scheib S and Baltes C 2013 Optimized Varian aSi portal dosimetry: development of datasets for collective use *J Appl Clin Med Phys* **14** 82-99
[25] Granfors P R and Aufrichtig R 2000 Performance of a 41X41-cm2 amorphous silicon flat panel x-ray detector for radiographic imaging applications *Med Phys* **27** 1324-31
[26] Myronakis M, Star-Lack J, Baturin P, Rottmann J, Morf D, Wang A, Hu Y-H, Shedlock D and Berbeco R I 2017 A novel multilayer MV imager computational model for component optimization *Med Phys* **44** 4213-4222
[27] Mijnheer B 2017 *Clinical 3D Dosimetry in Modern Radiation Therapy* (Boca Raton: CRC Press.
[28] Herman M G, Balter J M, Jaffray D A, McGee K P, Munro P, Shalev S, Van Herk M and Wong J W 2001 Clinical use of electronic portal imaging: report of AAPM Radiation Therapy Committee Task Group 58 *Med Phys* **28** 712-37
[29] Deshpande S, Xing A, Holloway L, Metcalfe P and Vial P 2014 Dose calibration of EPIDs for segmented IMRT dosimetry *J Appl Clin Med Phys* **15** 103-118
[30] Greer P B, Cadman P, Lee C and Bzdusek K 2009 An energy fluence-convolution model for amorphous silicon EPID dose prediction *Med Phys* **36** 547-55
[31] Kim S, Palta J R and Zhu T C 1998 The equivalent square concept for the head scatter factor based on scatter from flattening filter *Phys Med Biol* **43** 1593-1604